Suberoylanilide hydroxamic acid alleviates orthotopic liver transplantation-induced hepatic ischemia-reperfusion injury by regulating the AKT/GSK3β/NF-κB and AKT/mTOR pathways in rat Kupffer cells

JINGYUAN WANG[1*], MINGHUA DENG[1*], HAO WU[1], MENGHAO WANG[1], JIANPING GONG[1], HE BAI[1], YAKUN WU[2], JUNJIANG PAN[3], YONG CHEN[4] and SHENGWEI LI[1]

[1]Department of Hepatobiliary Surgery, Second Affiliated Hospital of Chongqing Medical University, Chongqing 400010; [2]Department of Hepatobiliary Surgery, Suining Central Hospital, Suining, Sichuan 629000; [3]Department of General Surgery, Second People's Hospital of Yibin City, Yibin, Sichuan 644000; [4]Department of Hepatobiliary Surgery, First Affiliated Hospital of Chongqing Medical University, Chongqing 400042, P.R. China

Abstract. Multiple mechanisms are involved in regulating hepatic ischemia-reperfusion injury (IRI), in which Kupffer cells (KCs), which are liver-resident macrophages, play critical roles by regulating inflammation and the immune response. Suberoylanilide hydroxamic acid (SAHA), a pan-histone deacetylase inhibitor, has anti-inflammatory effects and induces autophagy. To investigate whether SAHA ameliorates IRI and the mechanisms by which SAHA exerts its effects, an orthotopic liver transplantation (OLT) rat model was established after treatment with SAHA. The results showed that SAHA effectively ameliorated OLT-induced IRI by reducing M1 polarization of KCs through inhibition of the AKT/glycogen synthase kinase (GSK)3β/NF-κB signaling pathway. Furthermore, the present study found that SAHA upregulates autophagy 5 protein (ATG5)/LC3B in KCs through the AKT/mTOR signaling pathway and inhibition of autophagy by knockdown of ATG5 in KCs partly impaired the protective effect of SAHA on IR-injured liver. Therefore, the current study demonstrated that SAHA reduces M1 polarization of KCs by inhibiting the AKT/GSK3β/NF-κB pathway and upregulates autophagy in KCs through the AKT/mTOR signaling pathway, which both alleviate OLT-induced IRI. The present study revealed that SAHA may be a novel treatment for the amelioration of OLT-induced IRI.

Introduction

Hepatic ischemia-reperfusion injury (HIRI) remains a major cause of damage that is associated with several liver diseases and hepatic surgery, which affects the outcomes of hepatic operations and other liver diseases related to HIRI (1,2). Complex mechanisms are involved in HIRI and studies indicate that Kupffer cells (KCs), which are liver-resident macrophages, play a crucial role in the inflammatory response in several hepatic diseases (3-6). Two well-known KC phenotypes, M1 and M2, have different functions in HIRI; M1-polarized KCs exacerbate IR-induced damage to the liver by producing proinflammatory cytokines such as TNF-α and interleukin (IL)-1β, while anti-inflammatory cytokines, such as IL-10 and TGF-β, are produced by M2-polarized KCs and protect hepatocytes against IR injury (7-9). Therefore, increasing the number of M2 cells or reducing the M1 phenotype of KCs may help to ameliorate HIRI.

Autophagy is a conserved intracellular self-digestion process that eliminates damaged organelles and senescent proteins, in which autophagolysosomes created by the fusion of autophagosomes and lysosomes play a crucial role (10). Autophagy plays either a protective or detrimental role under different conditions, making it a 'double-edged sword' for stressed cells (11). The role of autophagy in HIRI remains controversial and depends on the treatment and how the model is established (warm or cold) (12-14). Studies have shown that autophagy plays a protective role in orthotopic liver transplantation (OLT)-induced IRI. Nakamura *et al* (15) demonstrated that HO-1/Sirt1-mediated autophagy contributes to ameliorating OLT-induced IRI in mice and humans. Zaouali *et al* (16) confirmed the hepatoprotective effect of AMPK-dependent

Correspondence to: Professor Yong Chen, Department of Hepatobiliary Surgery, First Affiliated Hospital of Chongqing Medical University, 1 Youyi Road, Yuanjiagang, Yuzhong, Chongqing 400042, P.R. China
E-mail: doctorcy007@163.com

Professor Shengwei Li, Department of Hepatobiliary Surgery, Second Affiliated Hospital of Chongqing Medical University, 76 Linjiang Road, Yuzhong, Chongqing 400010, P.R. China
E-mail: 300383@hospital.cqmu.edu.cn

Key words: suberoylanilide hydroxamic acid, liver transplantation, ischemia reperfusion injury, autophagy, Kupffer cells

autophagy in OLT-induced IRI. During HIRI, classically activated KCs (M1) damage the liver tissue not only by releasing reactive oxygen species and inflammatory cytokines but also by attracting other inflammatory cells to amplify these negative effects, and a previous study showed that autophagy plays a protective role by downregulating the cellular inflammatory response (17). In the livers of high-fat diet-fed mice, the loss of autophagy promotes lipopolysaccharide (LPS)-induced M1 polarization of KCs (18). Similarly, increased levels of IL-1β and IL-18 in LC3B knockout macrophages were observed in a sepsis mouse model, which revealed the protective role of autophagy in macrophage-related inflammation, but whether autophagy protects the liver from cold ischemia reperfusion remains to be elucidated (19).

Suberoylanilide hydroxamic acid (SAHA) is a pan-histone deacetylase inhibitor that has been applied clinically for the treatment of cancers for numerous years (20) and has also been shown to have anti-inflammatory effects on colitis and attenuate con A-induced acute hepatic injury (21,22). Choi *et al* (23) demonstrated that SAHA downregulates proinflammatory factor levels in plasma and inhibits responses of peripheral blood mononuclear cells to Toll-like receptor 4 (TLR4). Moreover, SAHA protects cardiomyocytes against IRI in an autophagy-dependent manner (24). Recent evidence suggests that SAHA affects the formation of autophagosomes and promotes autophagy (25). However, the role of SAHA in cold HIRI remains unclear and so a model of cold HIRI and SAHA pretreatment was established to investigate its effect on the IR-injured liver.

Studies have demonstrated that SAHA promotes autophagy of several cell models by downregulating AKT/mTOR signaling, which is one of the classical pathways involved in regulating cellular autophagy (26-29). AKT is a well-studied factor that functions in several models of diseases and positively regulates the phosphorylation of NF-κB, thus enhancing M1 polarization of macrophages (30,31). AKT also phosphorylates glycogen synthase kinase 3β (GSK3β), which is a conserved kinase that negatively regulates the activity of NF-κB. Cremer *et al* (32) demonstrated that GSK3β regulates the *Burkholderia cenocepacia*-mediated inflammatory in phagocytes through the PI3K/AKT/GSK3β/NF-κB pathway. Therefore, whether SAHA influences the AKT/GSK3β/NF-κB pathway in KCs and whether AKT/mTOR signaling is involved in SAHA-induced upregulation of KC autophagy was investigated.

Materials and methods

Animals and OLT in rats. The animal experiments involved in this study were in accordance with the National Institutes of Health Guide for the Care and Use of Laboratory Animals and approved by the Ethics Committee of the Second Affiliated Hospital of Chongqing Medical University (Chongqing, China). Sprague-Dawley (SD) rats (male, 250-300 g, 8-10 weeks old) were obtained from Chongqing Medical University Experimental Animal Center (Chongqing, China) and were selected as both donors and recipients. The animals were housed under specific pathogen-free conditions with an ambient temperature of 25°C, a controlled humidity of 50% and a 12 h light-dark cycle and were provided water and standard chow *ad libitum*. To establish an OLT model,

phenobarbital sodium was used to anesthetize both of the donor or recipient rats at a dose of 60 mg/kg body weight via intra-peritoneal injection (33), and the modified Kamada's two cuff technique (34) was used.

KC isolation. A total of 36 SD rats (male, 250-300 g) were sacrificed for the isolation of KCs, which was performed as described previously (35). The rats were anesthetized with phenobarbital sodium at a dose of 60 mg/kg body weight via intra-peritoneal injection and all of the rats used in the current research were euthanized by exsanguination from the inferior vena cava under sevoflurane anesthesia (3-4%). Electrocardiographic monitoring was used to verify death. After laparotomy, the livers were softened and yellowed by perfusion of 0.05% collagenase type IV through the portal vein, and then the liver was homogenized and filtered with a 200 mesh stainless steel screen. Subsequently, the suspension was centrifuged twice at 300 x g (4°C) for 5 min to remove the residual enzymatic solution as described previously (36). The supernatant was discarded, and the suspension was centrifuged at 50 x g (4°C) for 3 min to remove hepatocytes and other cells. Finally, the retained supernatant was centrifuged at 300 x g (4°C) for 5 min and the supernatant was discarded. The isolated KCs were plated and cultured with RPMI 1640 (Gibco; Thermo Fisher Scientific, Inc.) containing 10% fetal bovine serum (Hyclone, GE Healthcare Life Sciences) and 100 U/ml penicillin/streptomycin (Sigma-Aldrich; Merck KGaA) in a humidified atmosphere at 37°C and 5% CO_2. Primary KCs were identified by CD68 staining using immunofluorescence and flow cytometry.

Establishment of the rat HIRI model with ATG5 knockdown in KCs. Adeno-associated virus expressing ATG5-short hairpin (sh)RNA (AAV-ATG5-shRNA) and a control virus (scramble) were obtained from HanBio Biotechnology Co., Ltd. To obtain the KCs with ATG5 knockdown, the wild-type rats were injected with AAV-ATG5-shRNA or scramble (3×10^{12} vector genomes/kg) 30 days before liver transplantation via the tail vein. The mRNA and protein levels of ATG5 were measured by RT-qPCR and western blotting, respectively. To deplete KCs in the donor livers, clodronate liposomes (CLs) were used as before (37). Then KCs (2×10^7 cells) that were isolated from the liver tissue of AAV-ATG5-shRNA- or scramble-treated rats, were injected into recipients via the portal vein during OLT (38).

Experimental groups
In vivo. The rats were randomly divided into Sham group (n=5), IR group (n=5), IR+dimethyl sulfoxide treatment group (IR+DMSO, n=5), IR+SAHA treatment group (IR+SA, n=5), IR+SAHA+CLs treatment group (IR+SA+CL, n=5), IR+SAHA+chloroquine treatment group (IR+SA+CQ, n=5), IR+Scramble-shRNA treatment group (IR+Scramble, n=5), and IR+SAHA+ATG5-shRNA treatment group (IR+SA+ATG5-shRNA, n=5). For the Sham group, the rats received an abdominal incision and exposure of the liver vasculature. For the IR group, the grafts received 24 h of reperfusion after OLT without additional treatment. For the IR+SA group, the donors and recipients were both intraperitoneally injected with a dose of 50 mg/kg SAHA

(MedChemExpress) 12 h prior to operation, and the recipients continued to receive 50 mg/kg SAHA q12 h right from reperfusion via intra-peritoneal injection (39). For the IR+SA+CL group, CL (Encapsula NanoSciences) were injected into the donors at a dose of 4 μl/g body weight via the tail vein 48 h prior to surgery according to the manufacturer's protocol (37). Depletion of KCs were verified by using flow cytometry and immunohistochemistry, respectively. For the IR+SA+CQ group, 60 mg/kg CQ (Sigma-Aldrich; Merck KGaA) dissolved in PBS was injected into both of the donors and recipients 1 h prior to surgery (40). For the IR+SA+ATG5-shRNA group, the technique described above in the 'establishment of the rat HIRI model with ATG5 knockdown in KCs' was used. IR and SA treatment were performed as described before. For the vehicle-treatment groups, equal volumes of DMSO, liposomes or Scramble-shRNA were administered via the same routes as the respective drug treatments. No effects of these vehicles on liver function were found.

In vitro assays. KCs were randomly divided into Normal group, LPS (Sigma-Aldrich; Merck KGaA) treatment group, LPS+DMSO treatment group, LPS+SAHA treatment group (LPS+SA), LPS+Scramble-siRNA treatment group (LPS+Scramble), and LPS+SAHA+ATG5-siRNA treatment group (LPS+SA+ATG5-siRNA). In the Normal group, KCs were cultured with no additional treatment. In the LPS group, KCs were cultured with LPS (100 ng/ml) for 6 h (41). In the LPS+SA group, LPS-stimulated KCs were cultured with SAHA (3 μM) for 24 h (41). In the LPS+SAHA+ATG5-siRNA group, ATG5-siRNA (sense 5'-CAUGUGUGAAGGAAGCUG ATT-3', antisense 5'-UCAGCUUCCUUCACACAUGTT-3') or scrambled-siRNA (sense UUCGCUGAAGGUGCCACG CTT, antisense ACACGUCAUGCUCGGCGAGTT) was mixed with Lipofectamine 2000 (Invitrogen; Thermo Fisher Scientific, Inc.) at a final concentration of 50 nM according to the manufacturer's protocol. After transfection at 37°C for 48 h, KCs were treated with LPS and SAHA as described before, and the silencing efficiency was checked by western blotting. The sequences of ATG5-siRNA were determined based on a previous reference (42). For the vehicle-treatment group, 0.1% DMSO or scramble-siRNA was added to the medium in the same volume and at the same time point as the respective reagent treatments.

Hematoxylin and eosin (H&E) staining. H&E staining was performed according to the manufacturer's protocol (Beyotime Institute of Biotechnology). Paraffin sections (5-μm thick) of liver tissue were dewaxed and hydrated, followed by hematoxylin staining at 37°C for 5-10 min. Then, the paraffin sections were stained with eosin at 37°C for 30 sec-2 min. After dehydration, clearing and sealing, tissue damage and inflammation were observed under a light microscope (magnification, x400; Olympus Corporation). A total of six fields were captured for analysis per sample in blinded fashion. The severity of IRI was graded using Suzuki criteria (43).

Liver function examination. Serum was isolated from whole blood by centrifuging at 200 x g at 4°C for 10 min. The levels of serum alanine aminotransferase (sALT) and serum aspartate aminotransferase (sAST) were evaluated by using

an automatic biochemical meter (Beckman CX7; Beckman Coulter, Inc.).

TUNEL staining. TUNEL staining was performed according to the manufacturer's protocol (Wuhan Boster Biological Technology, Ltd.). Paraffin sections fixed with 4% paraformaldehyde for 1 h at room temperature were dewaxed, hydrated and digested with proteinase K for 15 min at 37°C. After washing 3 times for 2 min each, the tissue sections were incubated with a mixture of TdT, DIG-d-UTP and labeling buffer for 2 h at 37°C. After blocking for 30 min at 37°C, the sections were incubated with biotinylated anti-digoxigenin antibody at 37°C for 30 min, followed by incubation with SABC-FITC for 30 min. The nuclei were stained with DAPI at 37°C for 10 min. Finally, the fluorescence was detected by fluorescence microscopy (magnification, x400; Olympus Corporation). Results were scored semi-quantitatively by counting the number of positive cells in 6 fields per sample in a blinded fashion.

Flow cytometry analysis. To determine the ratio of M1 phenotype KCs, $1x10^6$ KCs were suspended in cell staining buffer before incubation with anti-CD68 (cat. no. ab201340; Abcam) and anti-CD86 (cat. no. ab213044; Abcam) antibodies at 4°C for 0.5 h. After washing 3 times with cell staining buffer, the samples were incubated with a FITC conjugation kit (Fast) (cat. no. ab188285; Abcam) or PE/Cy7 conjugation kit (cat. no. ab102903; Abcam) at 4°C in the dark for 30 min. After washing 3 times with cell staining buffer, the stained cells were acquired by a BD FACSCalibur and analyzed by using Cell Quest version 5.1 software (BD Biosciences).

Reverse transcription-quantitative PCR (RT-qPCR). Total RNA of liver tissue and cells was isolated by TRIzol reagent (Takara Bio, Inc.) and reverse transcribed into cDNA by using the PrimeScriptVR RT reagent kit with genomic DNA eraser (Takara Bio, Inc.). Reverse transcription of cDNA was conducted in a 20 μl reaction system: 10 μl mixture of 2 μl 5X gDNA Eraser Buffer, 1 μl gDNA Eraser, 1 μg Total RNA and RNase Free dH$_2$O was incubated at 42°C for 2 min and then stored at 4°C for subsequent reactions. Next, 1 μl PrimeScript RT Enzyme Mix I, 1 μl RT Primer Mix, 4 μl 5X PrimeScript Buffer 2 and 4 μl RNase Free dH$_2$O were added to the above mixture. Then the reverse transcription of cDNA was performed at 37°C for 15 min, 85°C for 5 sec, 4°C for 10 min and finally stored at -20°C. For qPCR, cDNA was mixed with primers and SYBR-Green (Takara Bio, Inc.) following the manufacturer's protocol and was then detected by a real-time detection system (Bio-Rad Laboratories, Inc.). The primers used were as follows: LC3B forward, 5'-TTAAGCCCC TACCAAGGCAA-3', reverse, 5'-CACTTGCATGGCACT CAGTTT-3'; P62 forward, 5'-TTGAGGCACCCCGTAAA GTC-3', reverse, 5'-TACATGGTGGCACCTACTGC-3'; ATG5 forward, 5'-CAGAAGCTGTTCCGTCCTGT-3', reverse, 5'-CCGTGAATCATCACCTGGCT-3'; and β-actin forward, 5'-CGTTGACATCCGTAAAGAC-3', reverse 5'-TGGAAG GTGGACAGTGAG-3' (Sangon Biotech Co., Ltd.). qPCR was conducted in a 25 μl reaction system, including 1 μl forward and 1 μl reverse primers, 12.5 μl SYBR-Green, 2 μl cDNA, and 8.5 μl dH$_2$O. The thermocycling conditions used for qPCR

were as follows: 95˚C for 30 sec, 40 cycles of 95˚C for 5 sec, 60˚C for 30 sec. All the samples were normalized to β-actin expression. The comparative method $2^{-\Delta\Delta Cq}$ (44) was used for the relative quantification of results and all experiments were repeated in triplicate.

Western blot analysis. KCs and liver tissue were treated with RIPA lysis buffer supplemented with protease inhibitors and phenylmethanesulfonyl fluoride (Beyotime Institute of Biotechnology). Protein concentrations were detected by a bicinchoninic acid protein quantitative kit (Beyotime Institute of Biotechnology) according to the manufacturer's protocol. A total of 30 µg protein was loaded per lane, separated using 10 or 12% SDS-PAGE and then electrotransferred onto polyvinylidene difluoride membranes. After blocking in 5% skim milk at 37˚C for 1 h, the membranes were incubated with primary antibodies at 4˚C overnight and then incubated with secondary antibody at 37˚C for 1 h. The bands were visualized by using an enhanced chemiluminescence kit (Thermo Fisher Scientific, Inc.) according to the manufacturer's protocol. All images were analyzed using ImageJ software, version 14.8 (National Institutes of Health). The primary antibodies used were as follows: TNF-α (1:1,000; cat. no. ab66579; Abcam), IL-1β (1:1,000; cat. no. ab9787; Abcam), IL-6 (1:1,000; cat. no. ab9324; Abcam), Bax [1:1,000; cat. no. 2772; Cell signaling Technology, Inc. (CST)], Bcl-2 (1:1,000; cat. no. ab196495; Abcam), caspase3 (1:1,000; cat. no. 9662; CST), cleaved-caspase3 (1:1,000; cat. no. 9664; CST), iNOS (1:1,000; cat. no. ab3523; Abcam), phosphorylated (p)-Akt (Ser473) (1:1,000; cat. no. 4060; CST), Akt (1:1,000; cat. no. 9272; CST), p-NF-κB p65 (1:1,000; cat. no. 3033; CST), NF-κB p65 (1:1,000; cat. no. 6956; CST), p-GSK3β (Ser9) (1:1,000; cat. no. 9336; CST), GSK3β (1:1,000; cat. no. ab93926; Abcam), p-mTOR (Ser2448) (1:1,000; cat. no. 5536; CST), mTOR (1:1,000; cat. no. 2972; CST), ATG5 (1:1,000; cat. no. 12994; CST), LC3B (1:1,000; cat. no. 3868; CST), P62 (1:1,000; cat. no. 23214; CST), and ATG16L1 (1:1,000; cat. no. 8089; CST).

Immunofluorescence staining. KCs were incubated with primary antibodies against LC3B (1:200; cat. no. #3868; CST) and CD68 (1:100; cat. no. ab201340; Abcam) at 4˚C overnight and then treated with FITC-conjugated goat anti-rabbit IgG (1:1,000; cat. no. ab6717; Abcam) for 1 h at room temperature in the dark. The nuclei were stained with DAPI at room temperature in the dark for 10 min, which was then detected by fluorescence microscopy (magnification, x200; Olympus Corporation). Six fields were blindly captured for analysis per sample. ImageJ software, version 14.8 (National Institutes of Health) was used to quantitate the levels of immunoreactivity.

Transmission electron microscopy (TEM). The autophagic vacuoles in KCs were viewed with TEM (magnification, x20,000; HITACHI HT-7700, Hitachi, Ltd.) at an accelerating voltage of 100 kV. After being treated with the appropriate reagents, the KCs were fixed with 2.5% glutaraldehyde at 4˚C for 24 h, and post-fixed with 1% osmium tetroxide at 4˚C for 2 h. Then, the samples were dehydrated with gradient ethanol, and embedded with 100% epoxy resin (cat. no. 45345-1L-F; Honeywell Fluka; Honeywell Research Chemicals) at 60˚C

for 24 h. Next, ultrathin sections at 70-nm thickness were prepared and stained with uranyl acetate and lead citrate. The preparation of the samples and the procedures were performed based on a previous reference (45). Autophagic vacuoles in 6 randomly selected fields per sample were counted. There were 5 sections for each specimen.

Statistical analysis. The statistical significance of differences between two groups was tested by Student's t test, while comparisons between more than two groups were performed by using one-way ANOVA followed by a Bonferroni post hoc test and the data are presented as the mean ± SD. GraphPad Prism 7 (GraphPad Software, Inc.) was used for data processing. P<0.05 was considered to indicate a statistically significant difference. Each experiment was repeated independently at least 3 times.

Results

SAHA protects the liver from cold IR in a KC-dependent manner. In this study, the impact of SAHA on the liver after cold IR was first investigated. SAHA pretreatment significantly attenuated damage caused by IRI compared with that of the sham group at 24 h, as indicated by reduced levels of sALT and sAST (Fig. 1A), and reduced hepatocellular damage (Fig. 1B and C) was found in the SAHA-treated group. Pretreatment with SAHA protected hepatocytes by reducing hepatocellular apoptosis, as demonstrated by the protein levels of cleaved-caspase3/caspase3, Bcl-2 and Bax (Fig. 1D and E). However, the protective effects of SAHA on IR-injured livers were diminished after depletion of KCs by CL (Fig. 1). Taken together, SAHA-mediated protection against cold liver IRI depends on KCs.

SAHA inhibits inflammation and promotes autophagy in grafts. To further investigate the effect of SAHA on the factors related to KC activation, the protein levels of proinflammatory factors and AKT/NF-κB p65 were detected, and the autophagy-related factors AKT/mTOR, ATG5, ATG16L1, LC3B, and P62 were also evaluated after IR insult. As shown in Fig. 2A and B, the proinflammatory factors IL-1β, TNF-α, and IL-6 were significantly increased after IR insult but were reversed by SAHA. AKT/NF-κB p65 was upregulated by IR insult but was reduced by SAHA (Fig. 2C and D). Consistent with the previous report that SAHA induces autophagy (25), SAHA also promoted autophagy in the grafts (Fig. 2E and F). As AKT/mTOR signaling is closely related to autophagy, the activity of AKT/mTOR was evaluated by western blotting and it was found that this pathway was downregulated by SAHA (Fig. 2C and D). These results indicate that SAHA regulates the inflammatory response after IR insult through the AKT/NF-κB pathway and promotes autophagy in grafts through the AKT/mTOR pathway, but whether SAHA promotes KC autophagy remains to be further investigated.

SAHA inhibits KC M1 polarization through the AKT/GSK3β/NF-κB pathway in vitro. To further investigate the effect of SAHA on the activation of KCs, LPS was used to induce sterile inflammation in KCs that were isolated from normal rats. CD68+CD86+ KCs were detected by flow cytom-
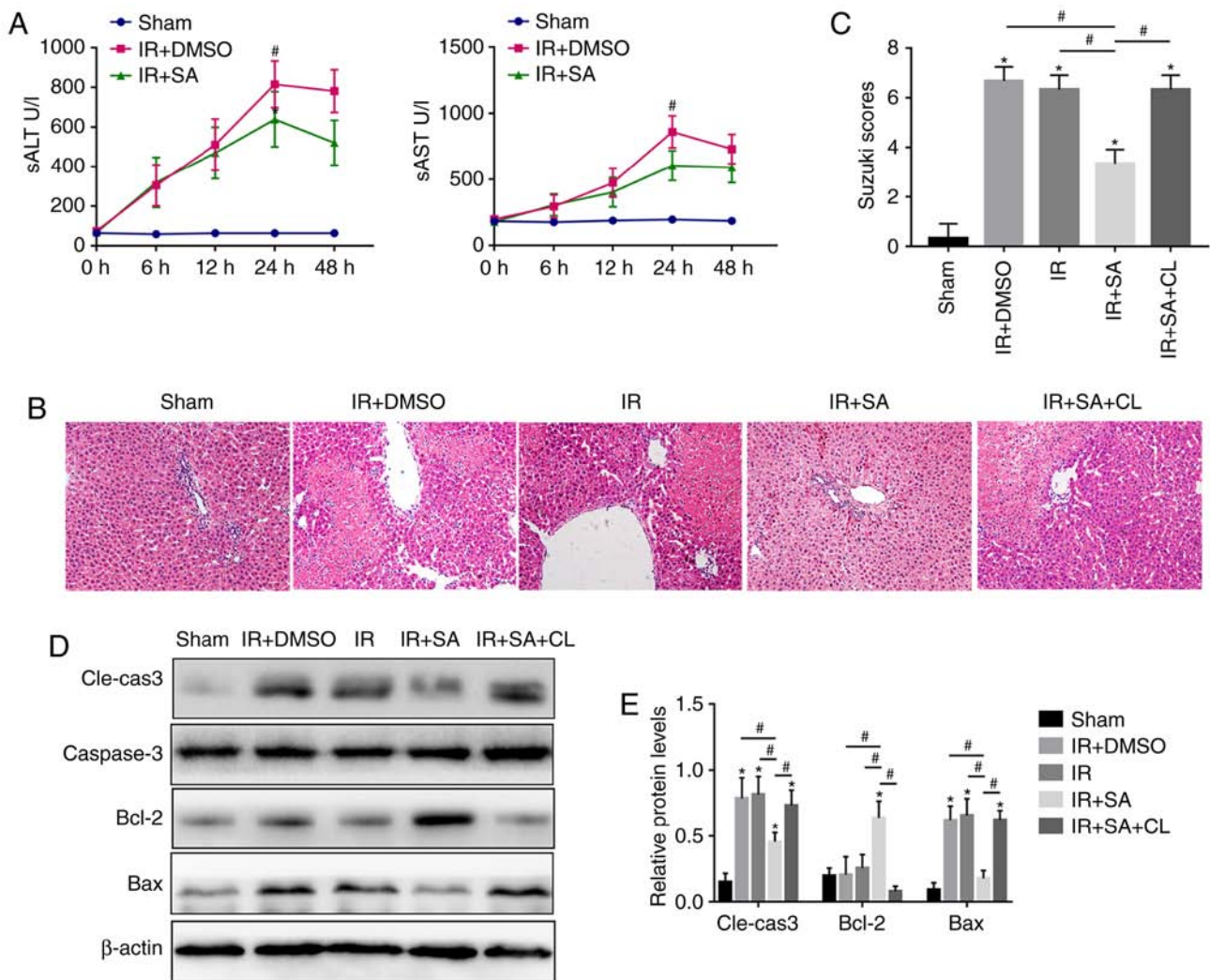
Figure 1. SAHA protects the liver from cold IR in a KC-dependent manner. (A) The serum concentrations of ALT and AST at 0, 6, 12, 24 and 48 h after OLT-induced IR in the Sham, IR+DMSO, IR, IR+SA and IR+SA+CL groups (n=5/group). (B) Images of hematoxylin and eosin (magnification, x400) staining showing the tissue damage in the grafts of different experimental groups at 24 h after IR and the (C) Suzuki score at 24 h after IR. (D) Western blot analysis of the expression of Cle-caspase3, caspase3, Bcl-2 and Bax. (E) Densitometric analysis of the western blot data. *P<0.05 vs. the Sham group and #P<0.05 vs. the IR+SA group. OLT, orthotopic liver transplantation; IR, ischemia reperfusion; DMSO, dimethyl sulfoxide; SA, suberoylanilide hydroxamic acid; CL, clodronate liposomes; KCs, Kupffer cells; Cle-caspase3, cleaved caspase3; sALT, serum alanine aminotransferase; sAST, aspartate transaminase, serum.

etry and the results showed that the ratio of M1 KCs in the LPS-treated group was much higher than that in the normal group but was downregulated in the SAHA-treated group (Fig. 3A and B). The downregulated protein level of iNOS, an M1 macrophage polarization marker, further confirmed that SAHA inhibited M1 polarization of KCs (Fig. 3C and D). Next, whether SAHA regulates M1 macrophage polarization through the AKT/GSK3β/NF-κB pathway was explored. As shown in Fig. 3C and D, the activity of NF-κB p65 was upregulated by LPS, which was accompanied by upregulated p-AKT (Ser473), but both were reduced by SAHA (Fig. 3C and D). Furthermore, LPS inhibited the activity of GSK3β but was activated by SAHA (Fig. 3C and D). These results suggest that SAHA reduces KC M1 polarization by inhibiting the AKT/GSK3β/NF-κB pathway.

SAHA promotes autophagy in KCs by inhibiting the AKT/mTOR pathway in vitro. Although SAHA promotes autophagy in liver grafts, whether it promotes autophagy in

KCs remains unknown. Therefore, autophagy-related factors were detected in isolated KCs from normal rat livers and the RT-qPCR results showed that ATG5 and LC3B were both increased in the SAHA-treated group compared with those in the LPS-treated group, accompanied by a reduction in P62 (Fig. 4A). SAHA-induced autophagy in KCs was further confirmed by western blotting (Fig. 4B-E). Furthermore, the immunofluorescence results showed that the fluorescence intensity in the SAHA-treated group was much higher than that in the LPS-treated group (Fig. 4F). Moreover, the TEM results showed that there were significantly more autophagic vacuoles in the LPS+SA group than in the Normal, LPS+DMSO and LPS groups (Fig. 5A). AKT/mTOR signaling is one of the classical pathways (26), and activation of AKT and mTOR was detected by western blotting, which showed that LPS-induced upregulation of p-mTOR (Ser2448) and p-AKT (Ser473) was abrogated by SAHA (Fig. 4B and C). These results indicate that SAHA promotes KC autophagy by downregulating the AKT/mTOR pathway.
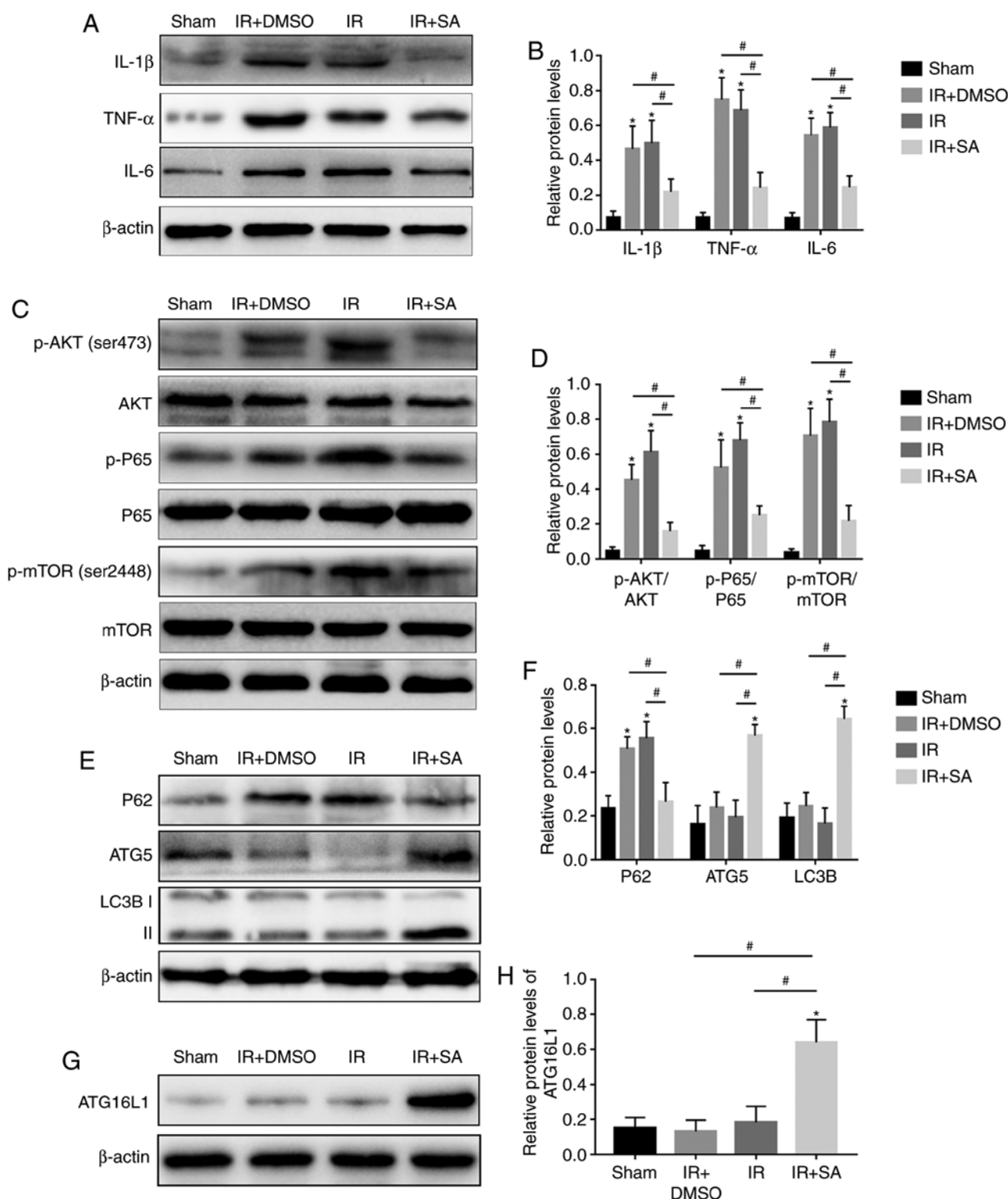
Figure 2. SAHA inhibits inflammation and promotes autophagy in grafts. (A) The protein levels of IL-1β, TNF-α and IL-6 in liver tissue were measured by western blotting. (B) Quantification of western blot data. (C) Western blot analysis of the protein levels of p-AKT, AKT, P-P65, P65, p-mTOR and mTOR in IR-livers. (D) Densitometric analysis of the western blot data. (E) The protein levels of P62, ATG5 and LC3B in the liver were detected by western blotting. (F) The relative protein levels of P62, ATG5 and LC3B. (G) The protein levels of ATG16L1 in the liver were detected by western blotting. (H) The relative protein levels of ATG16L1. *P<0.05 vs. the Sham group and $^#$P<0.05 vs. the IR+SA group. IL, interleukin; p-, phosphorylated; IR, ischemia reperfusion; DMSO, dimethyl sulfoxide; SA, suberoylanilide hydroxamic acid; CL, clodronate liposomes; ATG5, autophagy 5 protein.

To investigate the effect of autophagy on inflammation, KCs were isolated from normal rat livers and treated with ATG5-siRNA. As shown in Fig. 5B and C, the upregulated proinflammatory cytokines in LPS-treated KCs were downregulated by SAHA, and this effect was reversed by knockdown of ATG5 (Fig. 5B and C), which confirmed that the SAHA-mediated reduction in inflammation in KCs is partly dependent upon autophagy.
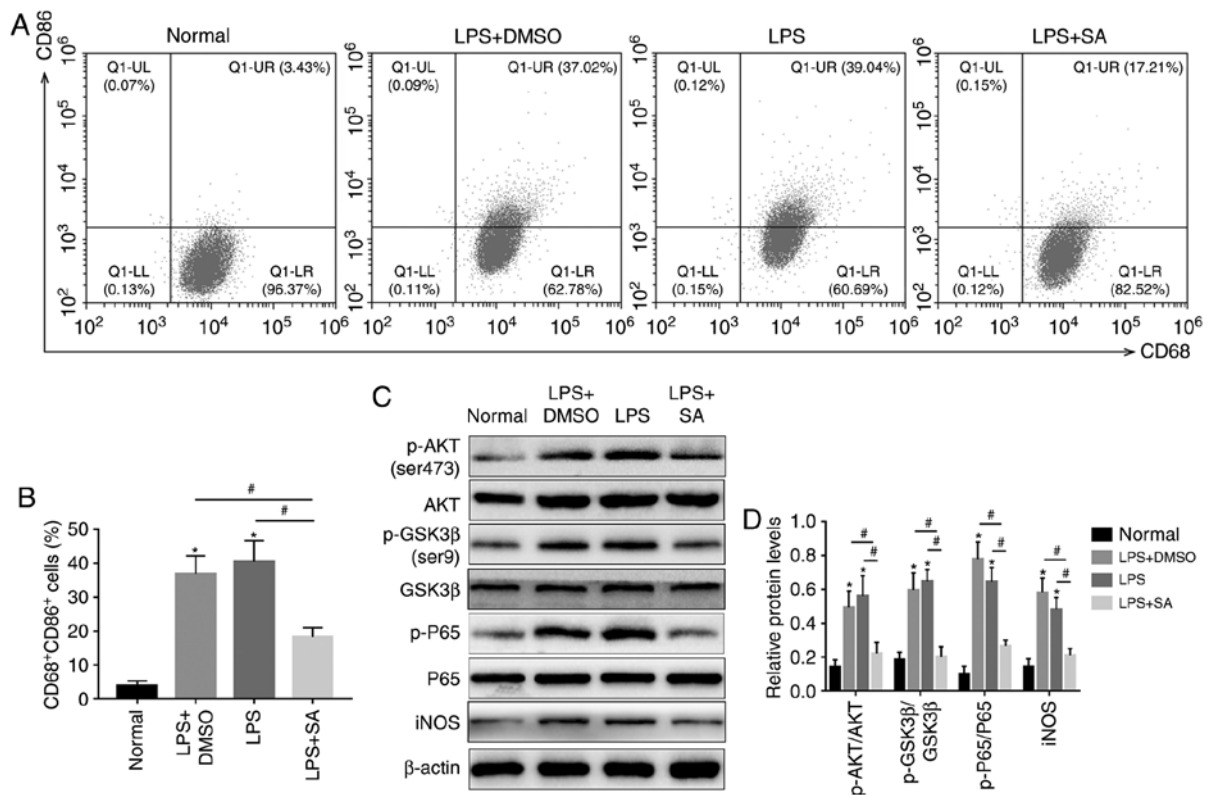
Figure 3. SAHA inhibits KC M1 polarization through the AKT/GSK3β/NF-κB pathway *in vitro*. (A) The ratio of CD68+CD86+ Kupffer cells was measured by flow cytometry and (B) analyzed. (C) Western blotting and (D) analysis of the protein levels of p-AKT, AKT, p-GSK3β, GSK3β, p-P65, P65 and iNOS. *$P<0.05$ vs. the normal group and #$P<0.05$ vs. the LPS+SA group. DMSO, dimethyl sulfoxide; SA, suberoylanilide hydroxamic acid; CL, clodronate liposomes; KCs, Kupffer cells; p-, phosphorylated; iNOS, inducible nitric oxide synthase; LPS, lipopolysaccharide; GSK, glycogen synthase kinase.

SAHA-mediated amelioration of liver injury depends on KC autophagy. Published studies have shown that autophagy plays a controversial role in liver ischemia reperfusion injury (11,46-48); therefore, the present study investigated the role of autophagy in the protective effect of SAHA on OLT-induced IRI by using the autophagy inhibitor CQ. The increased levels of serum ALT and serum AST in the CQ-treated group indicated that inhibition of autophagy partly impaired the protective effect of SAHA on OLT-induced IRI (Fig. 6A). Since SAHA protects the liver from cold IR in a KC-dependent manner, to further investigate the role of KC autophagy in SAHA-mediated protection against IR-induced liver injury, KC autophagy was downregulated by AAV-ATG5-shRNA *in vivo* as described previously (43) (Fig. 6B and C). The protective effect of SAHA on OLT-induced IRI was weakened in the AAV-ATG5-shRNA group, as increased levels of hepatocyte apoptosis were found in the SAHA+AAV-ATG5-shRNA group compared with those of the SAHA-treated group (Fig. 6D-G).

Discussion

Cold HIRI induced by OLT occurs early in liver transplantation and seriously decreases the survival rate of liver transplantation. The results of the current study demonstrate that the histone deacetylase inhibitor SAHA reduced the levels of proinflammatory cytokines and attenuated IR-induced liver injury in a KC-dependent manner. Although SAHA plays an anti-inflammatory role in various diseases (22,23,49), its

role in cold HIRI remains unclear. The present study showed that SAHA promoted autophagy in KCs by inhibiting the AKT/mTOR pathway, which contributes to ameliorating IR-induced liver injury. Moreover, SAHA reduced M1 polarization of KCs by inhibiting the AKT/GSK3β/NF-κB pathway.

Macrophages play a pivotal role in the initiation of innate and adaptive immune responses by shifting between M1 and M2 phenotypes. M1 macrophages release proinflammatory cytokines such as IL-1β and TNF-α, while M2 macrophages release anti-inflammatory cytokines such as TGFβ and IL10 (50). KC, the resident macrophages in the liver, are tightly associated with IR of the liver by triggering or suspending inflammation (51). In the present study, it was found that depletion of KCs impaired the protective effect of SAHA on the IR-liver, which indicates that SAHA attenuated OLT-induced IRI in a KC-dependent manner. During hepatic ischemia reperfusion, TLR4, a surface receptor on KCs, binds to danger signals such as damage-associated molecular patterns to activate KCs (52). In response to danger signal stimulation, activated KCs release proinflammatory and anti-inflammatory cytokines to play a dual role in modulating HIRI (53). A study performed by Leoni *et al* (22) showed that SAHA decreases proinflammatory cytokines released by LPS-stimulated peritoneal macrophages, but its effect on KCs in IRI remains to be elucidated.

Histone deacetylase inhibitors have been shown to induce autophagy and anti-exert anti-inflammatory effects *in vitro* and *in vivo* (54,55); SAHA ameliorates the outcomes of
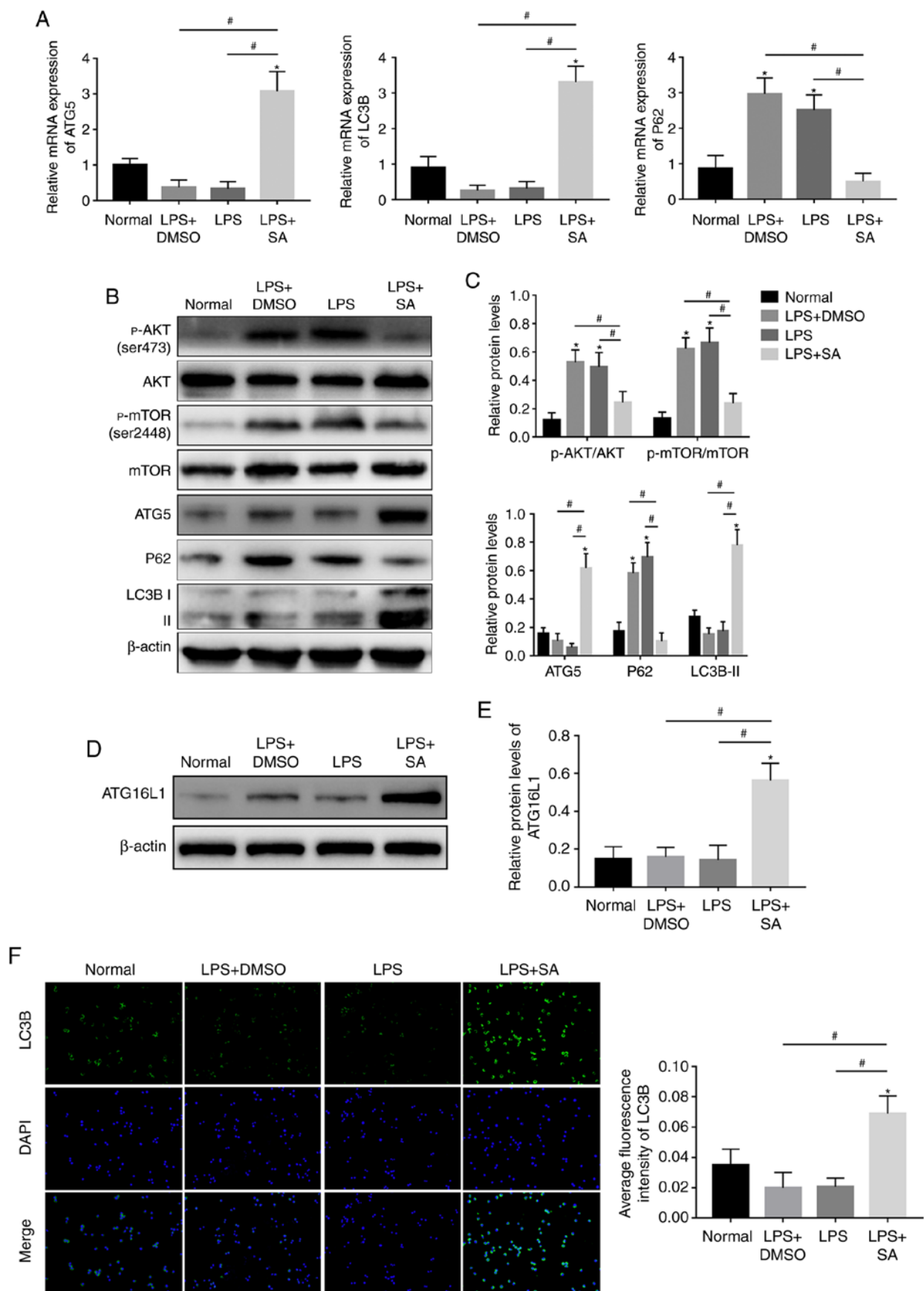
Figure 4. SAHA promotes autophagy in KCs by inhibiting the AKT/mTOR pathway *in vitro*. (A) The mRNA expression of ATG5, LC3B and P62 was analyzed by quantitative PCR. (B) Western blotting and (C) analysis was used to detect the expression of p-AKT, AKT, p-mTOR, mTOR, P62, ATG5 and LC3B. (D) Western blotting and (E) analysis was used to detect the expression of ATG16L1. (F) The fluorescence intensity of LC3B in KCs was detected by fluorescence microscopy and DAPI was used for nuclear staining (magnification, x200). *P<0.05 vs. the normal group and #P<0.05 vs. the LPS+SA group. DAPI, 4'6-diamidino-2-phenylindole; IR, ischemia reperfusion; SA, suberoylanilide hydroxamic acid; CL, clodronate liposomes; KCs, Kupffer cells; LPS, lipopolysaccharide; p, phosphorylated; ATG5, autophagy 5 protein.
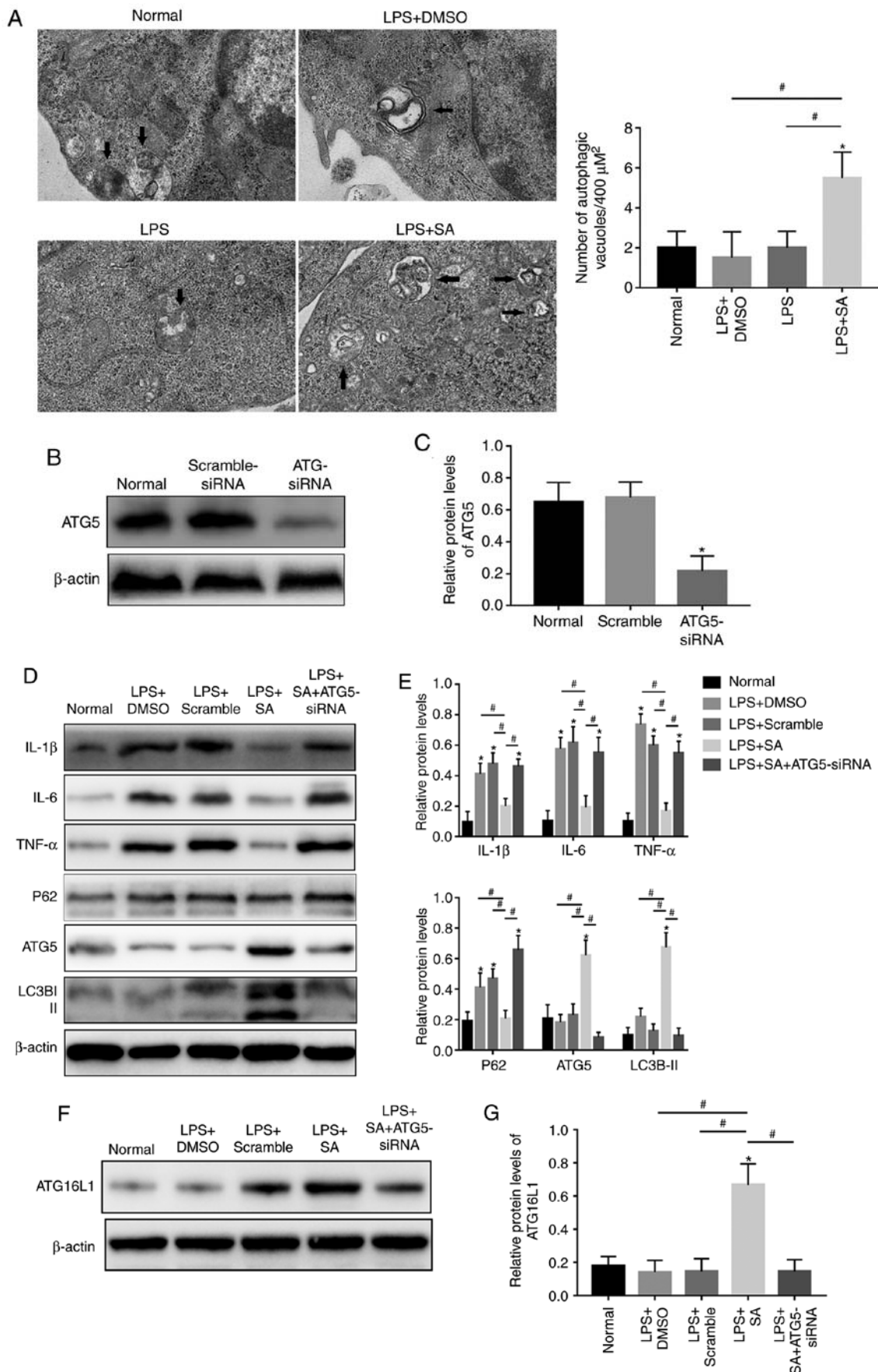
Figure 5. SAHA inhibits inflammatory cytokines in KCs in an autophagy-dependent manner. (A) Autophagic vacuoles (arrows) in KCs were observed by transmission electron micrograph (n=5/group; magnification, x20,000). (B) Western blotting and (C) analysis of the protein levels of ATG5 in KCs treated with or without ATG5-siRNA. (D) Western blotting and (E) analysis of the protein levels of IL-1β, IL6, TNFα, P62, ATG5 and LC3B in KCs. (F) Western blotting and (G) analysis of the protein levels of ATG16L1. *P<0.05 vs. the normal group and #P<0.05 vs. the LPS+SA group. IR, ischemia reperfusion; DMSO, dimethyl sulfoxide; SA, suberoylanilide hydroxamic acid; CL, clodronate liposomes; KCs, Kupffer cells; LPS, lipopolysaccharide; si, small interfering; IL, interleukin.
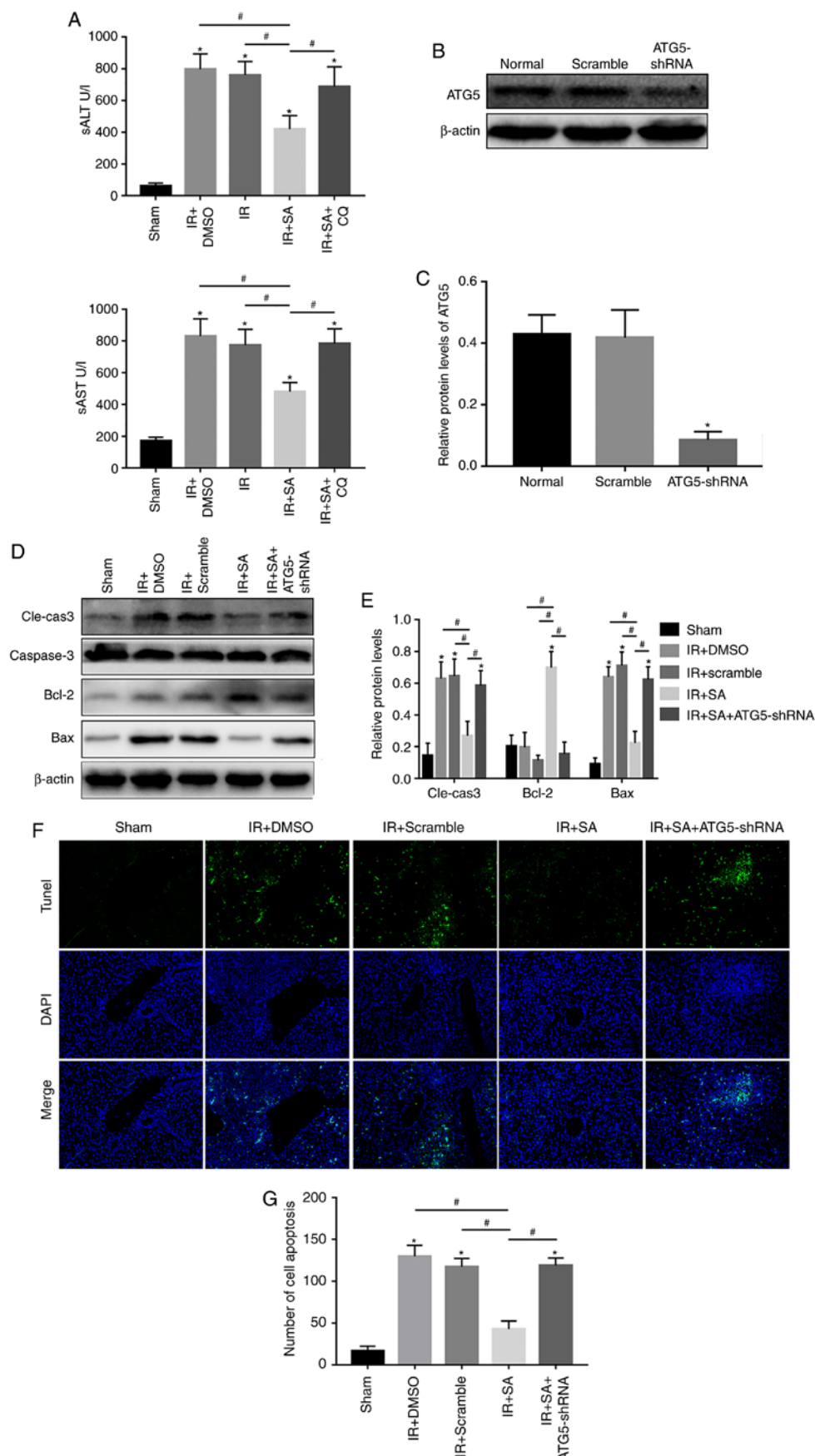
Figure 6. SAHA-mediated amelioration of liver injury depends on KC autophagy. (A) The serum concentrations of ALT and AST in each group. (B) The expression of ATG5 in KCs treated with or without AAV-ATG5-shRNA was examined by western blotting and (C) analyzed. (D) The expression of the apoptosis-related proteins Cle-caspase3, Bcl-2 and Bax in KCs treated with or without AAV-ATG5-shRNA was detected by western blotting and (E) analyzed. (F) Hepatocyte apoptosis was detected by TUNEL staining and DAPI was used for nuclear staining (magnification, x400). (G) Number of TUNEL-positive cells. $^*P<0.05$ vs. the Sham group and $^#P<0.05$ vs. the IR+SA group. CQ, chloroquine; TUNEL, terminal deoxynucleotidyl transferase-mediated dUTP-biotin nick end labeling assay; cle-caspase; cleaved caspase; KC, Kupffer cell; sh, short hairpin; ALT, alanine aminotransferase; AST, aspartate transaminase; IR, ischemia reperfusion.

cardiac ischemia reperfusion injury by inducing cardiomyo-cyte autophagy (24), but its role in cold liver IRI remains to be fully investigated. Autophagy is a highly conserved metabolic process that maintains cellular homeostasis by forming autophagic lysosomes to remove misfolded proteins and damaged organelles (56). Evidence indicates that autophagy is closely related to the inflammatory response; for example, proinflammatory cytokines IL-1α, IL-1β and type I interferon are increased in macrophages when autophagy is inhibited (57-59), while attenuated inflammation occurs in autophagy-overexpressing conditions (60,61). In the present study, it was found that SAHA reduced the upregulation of p-AKT and p-P65 after OLT, combined with the downregulation of M1 KC polarization in the SAHA-treated group *in vitro*. The current study detected whether AKT/GSK3β/NF-κB, a signaling pathway that participates in the inflammatory response of phagocytes (32), changed with SAHA treatment. The results showed that SAHA downregulated this pathway, which indicates that SAHA inhibits M1 polarization of KCs through the AKT/GSK3β/NF-κB signaling pathway. Moreover, SAHA promoted autophagy in KCs, accompanied by inhibition of AKT/mTOR signaling, which suggests that SAHA enhances autophagy in KCs through the AKT/mTOR pathway. Next, to explore the role of enhanced autophagy by SAHA in cold liver IRI, ATG5 in KCs was knocked down by AAV-ATG5-shRNA and the results showed that knock-down of ATG5 partly diminished the protective effect of SAHA on IR-injured livers, which is consistent with previous studies (57-59).

In conclusion, the present study shows that the antitumor drug SAHA effectively alleviates OLT-induced IRI. SAHA induces autophagy and inhibits M1 polarization of KCs, both of which contribute to ameliorating OLT-induced IRI. These findings provide evidence that SAHA may be an effective treatment for OLT-induced IRI.

Availability of data and materials

The datasets used and/or analyzed during the present study are available from the corresponding author upon reasonable request.

Authors' contributions

JW, MD, JG and SL designed the experiments and wrote the manuscript. JW, MD, HW and HB performed the experiments and analyzed the data. YC, JP and YW analyzed the data and revised the manuscript; they also provided assistance for the acquisition of the experimental funds. MW and SL contributed to the TEM experiments, and MW provided advice for the detection of ATG16L1. All authors read and approved the final manuscript.

Ethics approval and consent to participate

The animal experiments involved in this study were in accordance with the National Institutes of Health Guide for the Care and Use of Laboratory Animals and approved by the Ethics Committee of the Second Affiliated Hospital of Chongqing Medical University (Chongqing, China).

Patient consent for publication

Not applicable.

Competing interests

The authors declare that they have no competing interests.

References

1. Bavarsad K, Riahi MM, Saadat S, Barreto G, Atkin SL and Sahebkar A: Protective effects of curcumin against ischemia-reperfusion injury in the liver. Pharmacol Res 141: 53-62, 2019.
2. Linecker M, Frick L, Kron P, Limani P, Kambakamba P, Tschuor C, Langiewicz M, Kachaylo E, Tian Y, Schneider MA, *et al*: Exercise improves outcomes of surgery on fatty liver in mice: A novel effect mediated by the AMPK pathway. Ann Surg 271: 347-355, 2018.
3. Ju C and Tacke F: Hepatic macrophages in homeostasis and liver diseases: From pathogenesis to novel therapeutic strategies. Cell Mol Immunol 13: 316-327, 2016.
4. Takemura S, Azuma H, Osada-Oka M, Kubo S, Shibata T and Minamiyama Y: S-allyl-glutathione improves experimental liver fibrosis by regulating Kupffer cell activation in rats. Am J Physiol Gastrointest Liver Physiol 314: G150-G163, 2018.
5. Elsegood CL, Chan CW, Degli-Esposti MA, Wikstrom ME, Domenichini A, Lazarus K, van Rooijen N, Ganss R, Olynyk JK and Yeoh GC: Kupffer cell-monocyte communication is essential for initiating murine liver progenitor cell-mediated liver regeneration. Hepatology 62: 1272-1284, 2015.
6. Zigmond E, Samia-Grinberg S, Pasmanik-Chor M, Brazowski E, Shibolet O, Halpern Z and Varol C: Infiltrating monocyte-derived macrophages and resident kupffer cells display different ontogeny and functions in acute liver injury. J Immunol 193: 344-353, 2014.
7. Hu Y, Yang C, Shen G, Yang S, Cheng X, Cheng F, Rao J and Wang X: Hyperglycemia-triggered sphingosine-1-phosphate and sphingosine-1-phosphate receptor 3 signaling worsens liver ischemia/reperfusion injury by regulating M1/M2 polarization. Liver Transpl 25: 1074-1090, 2019.
8. Zheng D, Li Z, Wei X, Liu R, Shen A, He D, Tang C and Wu Z: Role of miR-148a in mitigating hepatic ischemia-reperfusion injury by repressing the TLR4 signaling pathway via targeting CaMKIIα in vivo and in vitro. Cell Physiol Biochem 49: 2060-2072, 2018.
9. Raptis DA, Limani P, Jang JH, Ungethüm U, Tschuor C, Graf R, Humar B and Clavien PA: GPR120 on Kupffer cells mediates hepatoprotective effects of ω3-fatty acids. J Hepatol 60: 625-632, 2014.
10. Allaire M, Rautou PE, Codogno P and Lotersztajn S: Autophagy in liver diseases: Time for translation? J Hepatol 70: 985-998, 2019.
11. Choi Y, Bowman JW and Jung JU: Autophagy during viral infection-a double-edged sword. Nat Rev Microbiol 16: 341-354, 2018.
12. Wang JH, Ahn IS, Fischer TD, Byeon JI, Dunn WA JR, Behrns KE, Leeuwenburgh C and Kim JS: Autophagy suppresses age-dependent ischemia and reperfusion injury in livers of mice. Gastroenterology 141: 2188-2199, 2011.

13. Rickenbacher A, Jang JH, Limani P, Ungethüm U, Lehmann K, Oberkofler CE, Weber A, Graf R, Humar B and Clavien PA: Fasting protects liver from ischemic injury through Sirt1-mediated downregulation of circulating HMGB1 in mice. J Hepatol 61: 301-308, 2014.

14. Wang JH, Behrns KE, Leeuwenburgh C and Kim JS: Critical role of autophage in ischemia/reperfusion injury to aged livers. Autophagy 8: 140-141, 2012.

15. Nakamura K, Kageyama S, Yue S, Huang J, Fujii T, Ke B, Sosa RA, Reed EF, Datta N, Zarrinpar A, *et al*: Heme oxygenase-1 regulates sirtuin-1-autophagy pathway in liver transplantation: From mouse to human. Am J Transplant 18: 1110-1121, 2018.

16. Zaouali MA, Boncompagni E, Reiter RJ, Bejaoui M, Freitas I, Pantazi E, Folch-Puy E, Abdennebi HB, Garcia-Gil FA and Roselló-Catafau J: AMPK involvement in endoplasmic reticulum stress and autophagy modulation after fatty liver graft preservation: A role for melatonin and trimetazidine cocktail. J Pineal Res 55: 65-78, 2013.

17. Quesnelle KM, Bystrom PV and Toledo-Pereyra LH: Molecular responses to ischemia and reperfusion in the liver. Arch Toxicol 89: 651-657, 2015.

18. Liu K, Zhao E, Ilyas G, Lalazar G, Lin Y, Haseeb M, Tanaka KE and Czaja MJ: Impaired macrophage autophagy increases the immune response in obese mice by promoting proinflammatory macrophage polarization. Autophagy 11: 271-284, 2015.

19. Nakahira K, Haspel JA, Rathinam VA, Lee SJ, Dolinay T, Lam HC, Englert JA, Rabinovitch M, Cernadas M, Kim HP, *et al*: Autophagy proteins regulate innate immune responses by inhibiting the release of mitochondrial DNA mediated by the NALP3 inflammasome. Nat Immunol 12: 222-230, 2011.

20. Sun Y, Sun Y, Yue S, Wang Y and Lu F: Histone deacetylase inhibitors in cancer therapy. Curr Top Med Chem 18: 2420-2428, 2018.

21. Glauben R, Batra A, Stroh T, Erben U, Fedke I, Lehr HA, Leoni F, Mascagni P, Dinarello CA, Zeitz M and Siegmund B: Histone deacetylases: Novel targets for prevention of colitis-associated cancer in mice. Gut 57: 613-622, 2008.

22. Leoni F, Zaliani A, Bertolini G, Porro G, Pagani P, Pozzi P, Donà G, Fossati G, Sozzani S, Azam T, *et al*: The antitumor histone deacetylase inhibitor suberoylanilide hydroxamic acid exhibits antiinflammatory properties via suppression of cytokines. Proc Natl Acad Sci USA 99: 2995-3000, 2002.

23. Choi SW, Gatza E, Hou G, Sun Y, Whitfield J, Song Y, Oravecz-Wilson K, Tawara I, Dinarello CA and Reddy P: Histone deacetylase inhibition regulates inflammation and enhances Tregs after allogeneic hematopoietic cell transplantation in humans. Blood 125: 815-819, 2015.

24. Xie M, Kong Y, Tan W, May H, Battiprolu PK, Pedrozo Z, Wang ZV, Morales C, Luo X, Cho G, *et al*: Histone deacetylase inhibition blunts ischemia/reperfusion injury by inducing cardiomyocyte autophagy. Circulation 129: 1139-1151, 2014.

25. Zhang J, Wang J, Zhou Z, Park JE, Wang L, Wu S, Sun X, Lu L, Wang T, Lin Q, *et al*: Importance of TFEB acetylation in control of its transcriptional activity and lysosomal function in response to histone deacetylase inhibitors. Autophagy 14: 1043-1059, 2018.

26. Chiao MT, Cheng WY, Yang YC, Shen CC and Ko JL: Suberoylanilide hydroxamic acid (SAHA) causes tumor growth slowdown and triggers autophagy in glioblastoma stem cells. Autophagy 9: 1509-1526, 2013.

27. Zhang P, Guo Z, Wu Y, Hu R, Du J, He X, Jiao X and Zhu X: Histone deacetylase inhibitors inhibit the proliferation of gallbladder carcinoma cells by suppressing AKT/mTOR signaling. PLoS One 10: e0136193, 2015.

28. Liu YL, Yang PM, Shun CT, Wu MS, Weng JR and Chen CC: Autophagy potentiates the anti-cancer effects of the histone deacetylase inhibitors in hepatocellular carcinoma. Autophagy 6: 1057-1065, 2010.

29. Hrzenjak A, Kremser ML, Strohmeier B, Moinfar F, Zatloukal K and Denk H: SAHA induces caspase-independent, autophagic cell death of endometrial stromal sarcoma cells by influencing the mTOR pathway. J Pathol 216: 495-504, 2008.

30. Wang X, Ikejima K, Kon K, Arai K, Aoyama T, Okumura K, Abe W, Sato N and Watanabe S: Ursolic acid ameliorates hepatic fibrosis in the rat by specific induction of apoptosis in hepatic stellate cells. J Hepatol 55: 379-387, 2011.

31. Fan Z, Li L, Li M, Zhang X, Hao C, Yu L, Zeng S, Xu H, Fang M, Shen A, *et al*: The histone methyltransferase Suv39h2 contributes to nonalcoholic steatohepatitis in mice. Hepatology 65: 1904-1919, 2017.

32. Cremer TJ, Shah P, Cormet-Boyaka E, Valvano MA, Butchar JP and Tridandapani S: Akt-mediated proinflammatory response of mononuclear phagocytes infected with *Burkholderia cenocepacia* occurs by a novel GSK3β-dependent, IκB kinase-independent mechanism. J Immunol 187: 635-643, 2011.

33. Liu A, Guo E, Yang J, Yang Y, Liu S, Jiang X, Hu Q, Dirsch O, Dahmen U, Zhang C, *et al*: Young plasma reverses age-dependent alterations in hepatic function through the restoration of autophagy. Aging Cell 17, 2018.

34. Kamada N and Calne RY: Orthotopic liver transplantation in the rat. Technique using cuff for portal vein anastomosis and biliary drainage. Transplantation 28: 47-50, 1979.

35. Li PZ, Li JZ, Li M, Gong JP and He K: An efficient method to isolate and culture mouse Kupffer cells. Immunol Lett 158: 52-56, 2014.

36. Zeng WQ, Zhang JQ, Li Y, Yang K, Chen YP and Liu ZJ: A new method to isolate and culture rat kupffer cells. PLoS One 8: e70832, 2013.

37. Piao X, Yamazaki S, Komazawa-Sakon S, Miyake S, Nakabayashi O, Kurosawa T, Mikami T, Tanaka M, Van Rooijen N, Ohmuraya M, *et al*: Depletion of myeloid cells exacerbates hepatitis and induces an aberrant increase in histone H3 in mouse serum. Hepatology 65: 237-252, 2017.

38. Pan G, Zhao Z, Tang C, Ding L, Li Z, Zheng D, Zong L and Wu Z: Soluble fibrinogen-like protein 2 ameliorates acute rejection of liver transplantation in rat via inducing Kupffer cells M2 polarization. Cancer Med Cancer Med 7: 3168-3177, 2018.

39. Yang J, He J, Ismail M, Tweeten S, Zeng F, Gao L, Ballinger S, Young M, Prabhu SD, Rowe GC, *et al*: HDAC inhibition induces autophagy and mitochondrial biogenesis to maintain mitochondrial homeostasis during cardiac ischemia/reperfusion injury. J Mol Cell Cardiol 130: 36-48, 2019.

40. Kang JW, Cho HI and Lee SM: Melatonin Inhibits mTOR-Dependent Autophagy during Liver Ischemia/Reperfusion. Cell Physiol Biochem 33: 23-36, 2014.

41. Hsieh IN, Liou JP, Lee HY, Lai MJ, Li YH and Yang CR: Preclinical anti-arthritic study and pharmacokinetic properties of a potent histone deacetylase inhibitor MPT0G009. Cell Death Dis 5: e1166, 2014.

42. Luo X, Wang D, Zhu X, Wang G, You Y, Ning Z, Li Y, Jin S, Huang Y, Hu Y, *et al*: Autophagic degradation of caveolin-1 promotes liver sinusoidal endothelial cells defenestration. Cell Death Dis 9: 576, 2018.

43. Li P, Liu H, Zhang Y, Liao R, He K, Ruan X and Gong J: Endotoxin tolerance inhibits degradation of tumor necrosis factor receptor-associated factor 3 by suppressing pellino 1 expression and the K48 ubiquitin ligase activity of cellular inhibitor of apoptosis protein 2. J Infect Dis 214: 906-915, 2016.

44. Livak KJ and Schmittgen TD: Analysis of relative gene expression data using real-time quantitative PCR and the 2(-Delta Delta C(T)) method. Methods 25: 402-408, 2001.

45. Sun HY, Hu YJ, Zhao XY, Zhong Y, Zeng LL, chen XB, Yuan J, Wu J, Sun Y, Kong W and Kong WJ: Age-related changes in mitochondrial antioxidant enzyme Trx2 and TXNIP-Trx2-ASK1 signal pathways in the auditory cortex of a mimetic aging rat model: Changes to Trx2 in the auditory cortex. FEBS J 282: 2758-2774, 2015.

46. Nakamura K, Kageyama S, Ito T, Hirao H, Kadono K, Aziz A, Dery KJ, Everly MJ, Taura K, Uemoto S, *et al*: Antibiotic pretreatment alleviates liver transplant damage in mice and humans. J Clin Invest 129: 3420-3434, 2019.

47. Liu H, Dong J, Song S, Zhao Y, Wang J, Fu Z and Yang J: Spermidine ameliorates liver ischaemia-reperfusion injury through the regulation of autophagy by the AMPK-mTOR-ULK1 signalling pathway. Biochem Biophys Res Commun 519: 227-233, 2019.

48. Liu A, Yang J, Hu Q, Dirsch O, Dahmen U, Zhang C, Gewirtz DA, Fang H and Sun J: Young plasma attenuates age-dependent liver ischemia reperfusion injury. FASEB J 33: 3063-3073, 2019.

49. Ratay ML, Balmert SC, Bassin EJ and Little SR: Controlled release of an HDAC inhibitor for reduction of inflammation in dry eye disease. Acta Biomater 71: 261-270, 2018.

50. Schmieder A, Michel J, Schönhaar K, Goerdt S and Schledzewski K: Differentiation and gene expression profile of tumor-associated macrophages. Semin Cancer Biol 22: 289-297, 2012.

51. Wang J, Koh HW, Zhou L, Bae UJ, Lee HS, Bang IH, Ka SO, Oh SH, Bae EJ and Park BH: Sirtuin 2 aggravates postischemic liver injury by deacetylating mitogen-activated protein kinasephosphatase-1. Hepatology 65: 225-236, 2017.

52. Tsung A, Klune JR, Zhang X, Jeyabalan G, Cao Z, Peng X, Stolz DB, Geller DA, Rosengart MR and Billiar TR: HMGB1 release induced by liver ischemia involves toll-like receptor 4 dependent reactive oxygen species production and calcium-mediated signaling. J Exp Med 204: 2913-2923, 2007.

53. Tasnim F, Xing J, Huang X, Mo S, Wei X, Tan MH and Yu H: Generation of mature kupffer cells from human induced pluripotent stemcells. Biomaterials 192: 377-391, 2019.

54. Zhang J, Ng S, Wang J, Zhou J, Tan SH, Yang N, Lin Q, Xia D and Shen HM: Histone deacetylase inhibitors induce autophagy through FOXO1-dependent pathways. Autophagy 11: 629-642, 2015.

55. Hancock WW, Akimova T, Beier UH, Liu Y and Wang L: HDAC inhibitor therapy in autoimmunity and transplantation. Ann Rheum Dis 71 (Suppl 2): i46-i54, 2012.

56. Yamamoto A and Yue Z: Autophagy and its normal and pathogenic states in the brain. Annu Rev Neurosci 37: 55-78, 2014.

57. Lee JP, Foote A, Fan H, Peral de Castro C, Lang T, Jones SA, Gavrilescu N, Mills KH, Leech M, Morand EF and Harris J: Loss of autophagy enhances MIF/macrophage migration inhibitory factor release by macrophages. Autophagy 12: 907-916, 2016.

58. Tal MC, Sasai M, Lee HK, Yordy B, Shadel GS and Iwasaki A: Absence of autophagy results in reactive oxygen species-dependent amplification of RLR signaling. Proc Natl Acad Sci USA 106: 2770-2775, 2009.

59. Castillo EF, Dekonenko A, Arko-Mensah J, Mandell MA, Dupont N, Jiang S, Delgado-Vargas M, Timmins GS, Bhattacharya D, Yang H, Hutt J, et al: Autophagy protects against active tuberculosis by suppressing bacterial burden and inflammation. Proc Natl Acad Sci USA 109: E3168-E3176, 2012.

60. Eisenberg T, Abdellatif M, Schroeder S, Primessnig U, Stekovic S, Pendl T, Harger A, Schipke J, Zimmermann A, Schmidt A, et al: Cardioprotection and lifespan extension by the natural polyamine spermidine. Nat Med 22: 1428-1438, 2016.

61. Sun Y, Yao X, Zhang QJ, Zhu M, Liu ZP, Ci B, Xie Y, Carlson D, Rothermel BA, Sun Y, et al: Beclin-1-dependent autophagy protects the heart during sepsis. Circulation 138: 2247-2262, 2018.